Following the progress of sintering by measuring viscosity and electrical resistivity variations

O. Lame, Sylvie Bourdineaud-Bordère, Dominique Denux, Didier Bouvard

FOLLOWING THE PROGRESS OF SINTERING BY MEASURING VISCOSITY AND ELECTRICAL RESISTIVITY VARIATIONS

Olivier Lame*, Sylvie Bordère, Dominique Denux** and Didier Bouvard***

***Laboratoire Génie Physique et Mécanique des Matériaux**
INPG, UMR CNRS 5010
BP 46, 38402 Saint Martin d'Hères Cedex

****Institut de Chimie de la Matière Condensée de Bordeaux, CNRS**
87, Avenue du Docteur Schweitzer
33608 Pessac Cedex

ABTRACT

The simplest way of characterising the advancement of sintering of a powder is to follow the variation of its relative density. However, sintering of dense compact, obtained for example by die pressing of iron-based powders, occurs with very low density changes, while, of course, the microstructure and the properties of the material strongly evolve. In this study, the progress of sintering is followed by a continuous measurement of two characteristics of the material throughout sintering: the electrical resistivity and the viscosity. The original techniques developed for the measurement are presented and the interest of the data obtained for the understanding and modelling of sintering is discussed.

INTRODUCTION

The state of a powder during a sintering cycle is classically characterised by its relative density. This parameter is easy to measure and it can represent the progress of sintering for many types of powders, in particular hard powders. Such powders generally exhibit a low relative density after compaction, typically around 0.5, whereas after sintering, the relative density can be close to 1. Physical and mechanical properties of the material are mainly related with density. Therefore, for a macroscopic characterisation, the relative density turns out to be a suitable parameter describing the irreversible evolution during sintering. All the numerical simulations based on continuum mechanics that aim at predicting shape changes of powder compacts during sintering use relative density as a unique internal variable in the constitutive equations [1-4].

However, for ductile powders submitted to prior compaction, this description is not adequate. Most often, the plastic deformation of the particles during compaction results in a high green density, typically above 90 % and the subsequent sintering does not significantly change the density although the material gets, of course, much stronger. This is the case for iron-based Distaloy AE powder studied here. Therefore, new parameters have to be found to characterise the irreversible changes of the material occurring during sintering.

Following the method defined by Cai et al.[10], several authors determined the viscosity of a powder during a sintering cycle from the jump in densification rate resulting from the application of a load upon the specimen. In particular, Lame et al. showed that the viscosity of Distaloy compacts strongly evolved throughout sintering [5]. On the other hand, Simchi, Danninger and al. [6,7,8] measured the electrical conductivity of iron-based powder compacts after different sintering times and also found that this physical property could characterise the microstructural changes during sintering.

In this paper, the evolution of both the electrical resistivity and the viscosity of Distaloy AE powder compacts are continuously measured during a sintering cycle. The electrical resistivity is measured with an original dilatometer that provides simultaneously the shrinkage and the resistivity of a sintering material. The viscosity is deduced from the results of a bending test performed in a dilatometer allowing the application of a load through the measurement rod. Two sintering progress parameters are defined from resistivity and viscosity data. The evolution of these parameters are then analysed and their interest for better understanding and modelling of the sintering of metal powders is discussed.

SHRINKAGE AND RESISTIVITY MEASUREMENTS

The experimental device developed to measure the shrinkage and the electrical resistivity of a specimen during a thermal cycle is presented in Figure 1. This device is based on a Netzsch differential dilatometer which allows the measurement of the difference in expansion or shrinkage between a specimen and a reference body (alumina) using an inductive displacement transducer. The four collinear probe method is used to determine the resistivity [9]. The resistivity, ρ, of the material is deduced from the tension U induced by a current source of intensity I from the relation :

$$\rho = \frac{U}{I}\frac{S}{L} \qquad (1)$$

where S is the surface of section perpendicular to the current lines and L is the distance between the two tension measurement wires. A nano-voltmeter is used for a best accuracy of voltage measurement. If the current source wires and tension measurement wires are positioned on a specimen side parallel to the direction of compaction, the axial resistivity is then obtained. If the four wires are positioned on a side perpendicular to the direction of compaction, the transverse resistivity is obtained.

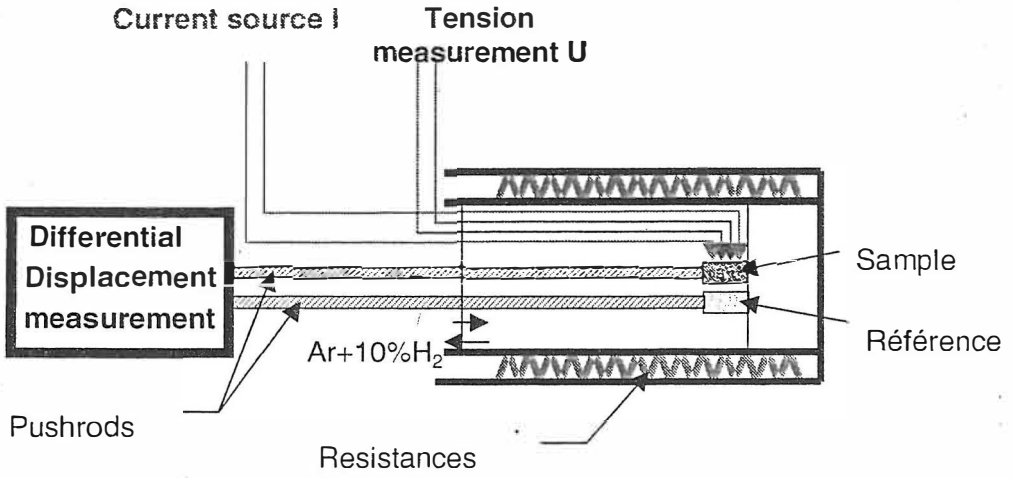

Figure 1. Schematics of the device developed to simultaneously measure the shrinkage and the electrical resistivity of a sample during a thermal cycle.

SHRINKAGE AND RESISTIVITY RESULTS

The samples were obtained from Distaloy AE powder (Fe + 1,5 % Cu, + 0,5 % Mo et 4 % Ni) mixed with 0,6 wgt.% of graphite. The powder was first compacted into a rigid die. For a compacting pressure of 750 MPa (resp. 400 MPa), the density of the compact was 7,08 g/cm^3 (resp. 6,5 g/cm^3) ± 0,05 g/cm^3. The compacts were then sintered under reducing Ar + 10 % H_2 atmosphere. The first thermal cycle was the following : heating at 10°C/min up to 1130°C, isothermal stage during 2 hours and a cooling at 10°C/min. The samples were parallelepipedic with 8 mm length, 4 mm width and 8 mm height (direction of compaction). Typical dilatometric results are reported in Figure 2 for specimens of density 6.5 g/cm^3 measured either in the compression direction and in a transverse direction. The beginning of the curves corresponds to the thermal expansion of the specimen. Until 800 °C, various phenomena, such as dewaxing or stress relaxation, happen. The slight perturbations marked with double arrows on the curves probably correspond to these effects. The $\alpha \rightarrow \gamma$ iron phase transformation occurs between 800 and 900°C. This transformation is likely much more complex than classical iron phase transformation due to alloying elements and during this period an anisotropy in strain appears. During the isothermal stage, the material shrinks equally in both directions. After cooling, the shrinkage is about 0.9 % in the direction of compaction and 0.75 % in the transverse direction. A second cycle with an isothermal stage at 1130°C of only a few minutes is applied to the same specimens. It can be observed the deformation is the same in both directions. It is noticeable that the strain has a much lower magnitude during phase transformation than during the same period in the first cycle.

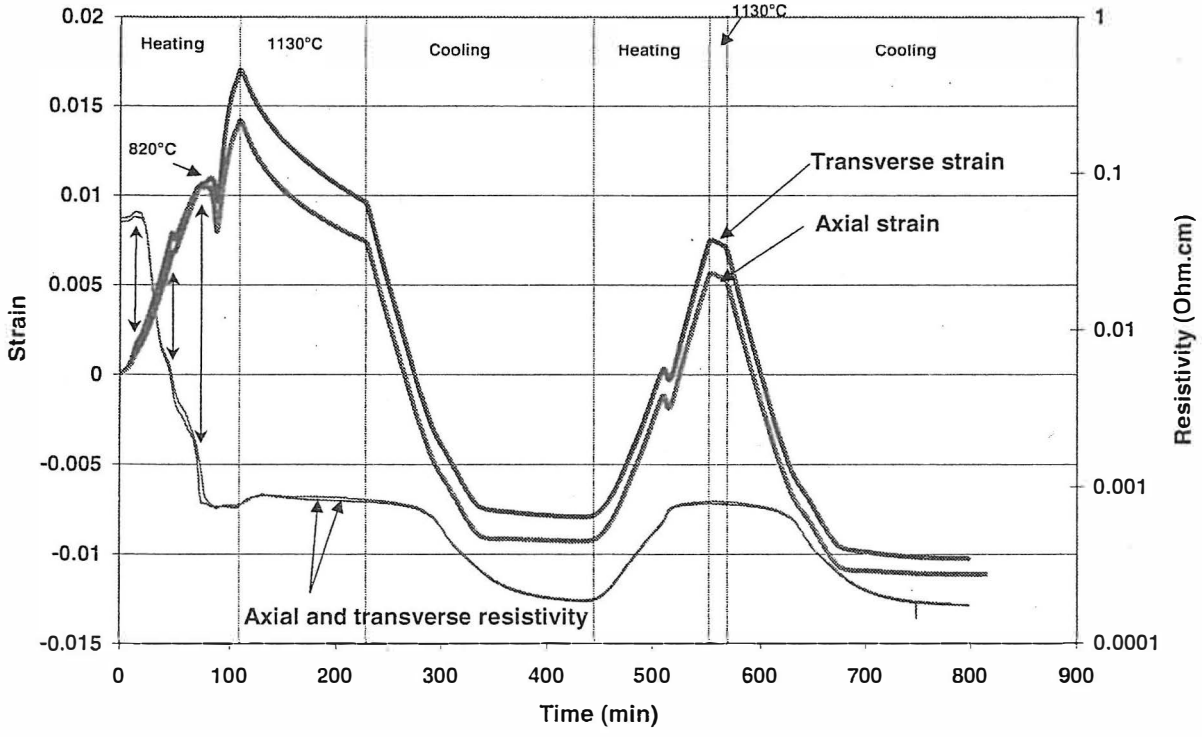

Figure 2 : Shrinkage and resistivity measurements of 6.5 g/cm^3 samples during two successive thermal cycles.

The results of resistivity measurement also appear in Figure 2. In the first cycle, the resistivity strongly decreases during heating. This variation is likely a consequence of the welding of interparticle contacts formed during compaction. The observed perturbations correspond to dewaxing, stress relaxation and phase transformation. Just before the isothermal stage, the resistivity has a value around 100 times lower than the initial value. During the isothermal stage, while the material shrinks, its resistivity weakly decreases. For this compacting pressure, no significant anisotropy in electrical resistivity is observed. During the second cycle resistivity changes are much more gentle and almost reversible. Therefore, they are supposed to be intrinsic variations of the resistivity of the sintered material versus temperature. In fact,

we assume that the irreversible evolutions of resistivity occurring after the first thermal treatment are negligible and that the material is thus at the thermodynamic equilibrium. This state will be called "final state" of sintering. The results obtained in the second cycle will be used to normalise the data obtained during the first cycle in order to describe the irreversible effects due to sintering.

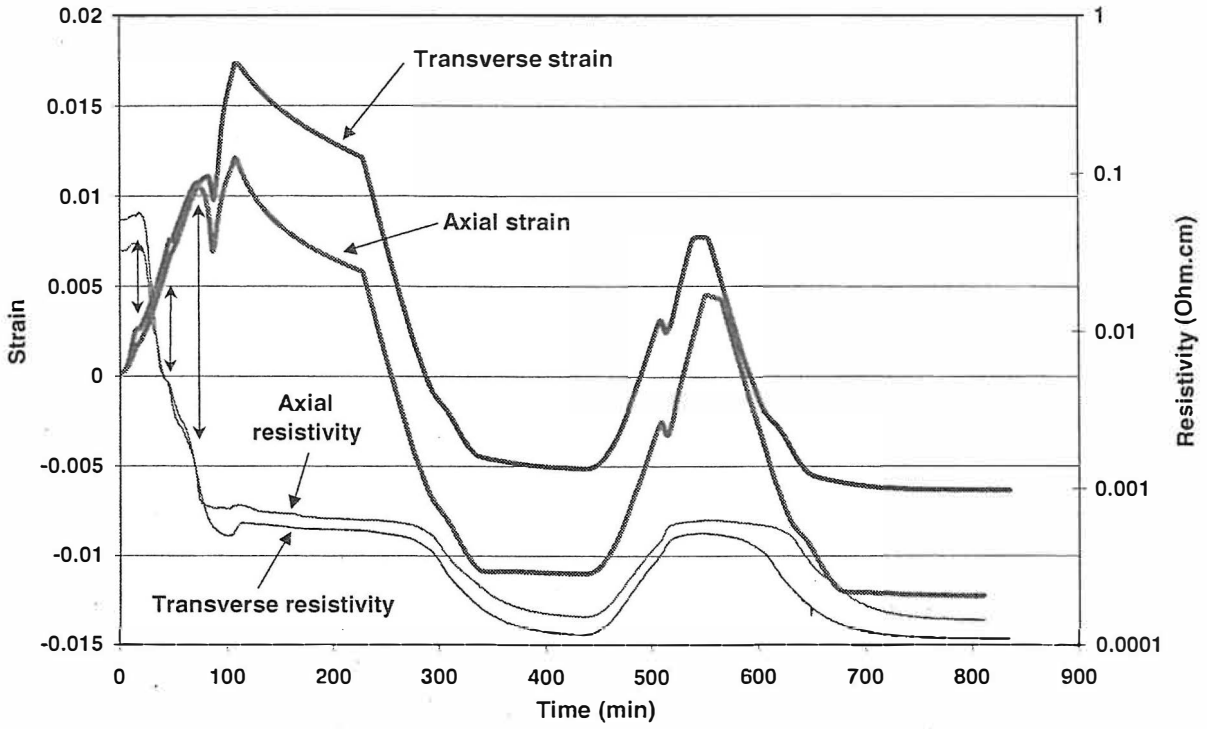

Figure 3 : Shrinkage and resistivity measurements of 7.1 g/cm^3 samples during two successive thermal cycles.

The same experiments are performed for two samples compacted at 750 MPa. The same tendencies are found. However, the anisotropy in shrinkage is more important during both heating and isothermal periods. After cooling, the shrinkage in the direction of compaction is twice the shrinkage in the transverse direction. Concerning electrical resistivity, a significant difference was measurable at the beginning of the experiment. The resistivity was 20 % lower in the compaction direction than in the transverse direction. This result can be understood since the contacts normal to the direction of compaction underwent higher stresses and then should be larger and tighter. Note that in the compaction direction the density gradient due to compaction could have an influence on the resistivity results. In the transverse direction the measurement is performed at the middle of the sample (close to the lowest density region). In this paper these parameters are not investigated. During phase transformation, an opposite difference between axial and transverse resistivity suddenly occurs and remains unchanged until the end of the test, including during the second cycle. So far we have not been able to explain this effect, which should be confirmed by further experiments.

For both tests, the resistivity found during the second cycle has been used as a reference to normalise the results obtained during the first cycle. Actually, as we preferred a parameter that mainly increases throughout sintering, we chose to use the normalised conductivity (inverse of resistivity). Figure 4 shows that the normalised conductivity strongly increases during heating until the beginning of the phase transformation, as contacting particles weld to each other. Then it gets about constant and exhibits a moderate increase during the isothermal period.

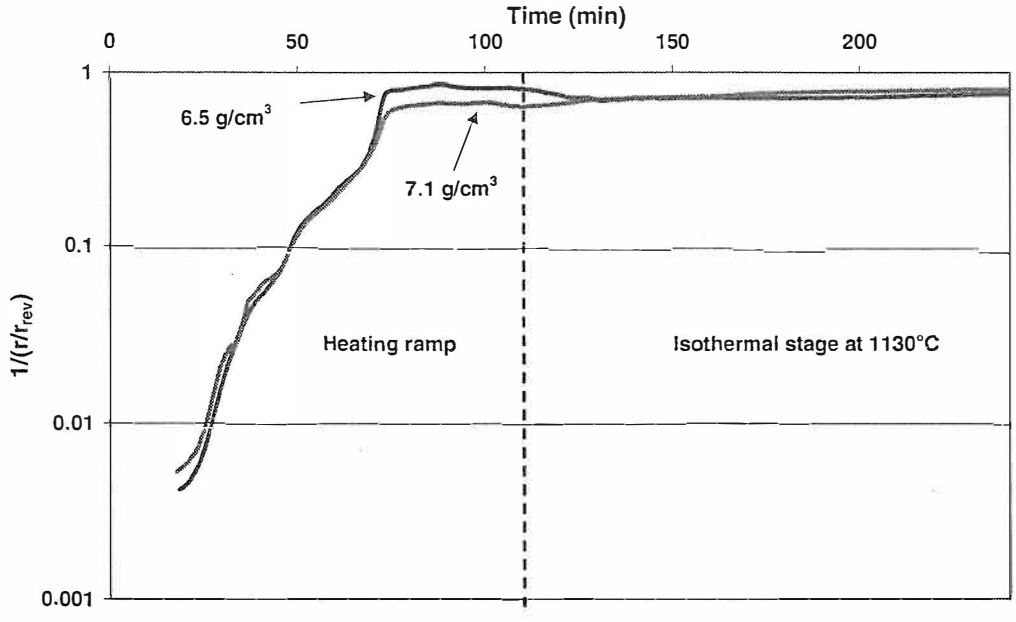

Figure 4. Normalised conductivity during the first thermal cycle.

VISCOSITY MEASUREMENT

The thermal cycle used for this measurement was close to a typical industrial cycle: heating at 40°C/min up to 1130°C, isothermal stage during 1 hour and rapid cooling. The samples were parallelepipedic with 15 mm length, 3 mm width and 2 mm height. During the thermal cycle, the sample is submitted to a bending test (Figure 5). The sample lies upon two far-apart supports spaced out of 12 mm and an alumina rod with a sharp edge is set on the middle of it. A load between 15 to 150 g is continuously applied and the deflection of the sample is deduced from the displacement of the rod. During such test, the preponderant stress is the normal stress in the horizontal direction. Then the viscosity obtained with the method described below is mainly representative of the behaviour of the material in the direction perpendicular the direction of compaction. It has been verified that the shrinkage due to free sintering was negligible in comparison with the deflection.

Two kinds of samples were tested. First, green compacts gave information on the evolution of the viscosity during the sintering cycle. Secondly, the viscosity of a sample previously sintered during 5 hours at 1130°C will be used as a reference to normalise the results obtained for the green sample. Such sample will be referred as a final state sample.

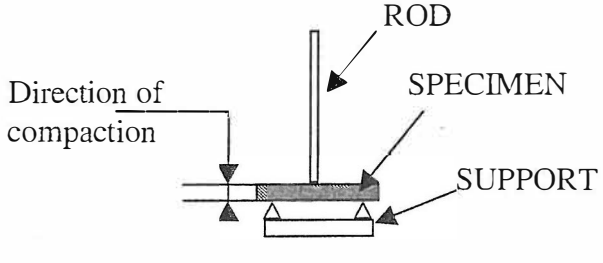

Figure 5 : Schematics of bending test device

VISCOSITY RESULTS

The classical experiment for measuring viscosity in the course of sintering consists in applying short compressive loading sequences [10, 11]. The viscosity is then deduced from the jump in strain rate induced by the load. In such a test, the stress state is perfectly defined and homogenous, thus the interpretation is straightforward. Conversely, during bending test, the state of stress is not complex. However, the major interest of this test is that it allows applying much higher stresses than compressive tests. For example, with a load of 150g, the maximum applied stress is around 6 MPa with the bending test whereas it would be very difficult the reach more than 0.2 MPa in compression test without using a sample with very small section area. For green samples, both methods could be used since the effect of a small stress is significant and can be measured with a good accuracy. Conversely, for highly sintered material, the viscosity is very high and then the effect of small stress is difficult to measure with accuracy. Consequently, the bending method is particularly useful in this case. Figure 6 and 7 show the deflection of two different samples, a green sample (a) and a sample in the final state (b).

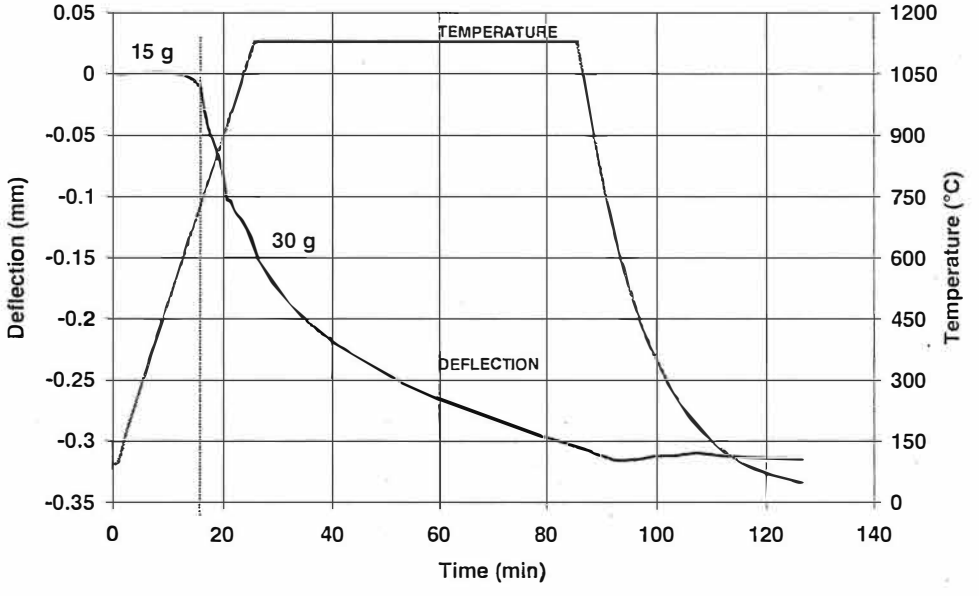

Figure 6 : Deflection measured during bending test a green compact (a)

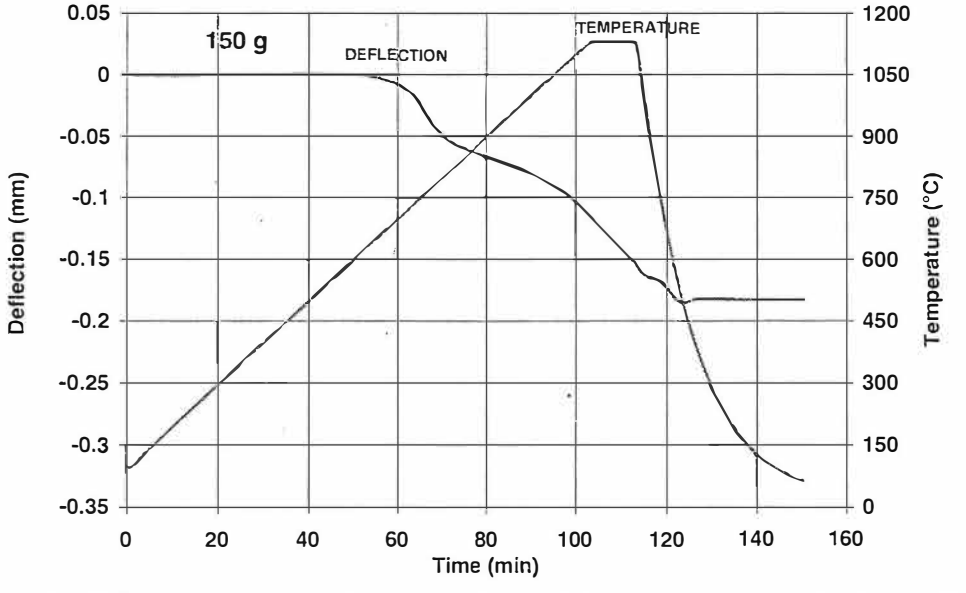

Figure 7 : Deflection measured during bending test for a material in the final state (b).

The sample (a) was submitted to the sintering cycle described above. Since the sample (a) had a very low mechanical resistance at the beginning of the test, 15 g was applied until 700°C and next 30 g until the end of the test. It can be seen that the deformation begins at around 600°C. Then the deflection increases continuously, strongly during the end of the heating period and more smoothly during the isothermal stage. The microstructure of sample (b) is supposed to be stable, thus its behaviour should to be only dependent on the temperature. Therefore, to increase the accuracy on the measurement of the temperature, the heating rate was decreased to 10°C/min. The applied load was 150 g. Even with a load 5 times higher than the one applied upon sample (a), the deflection is lower which means that the viscosity is much higher.

From these results, it is possible to deduce the viscosity at any time of the thermal cycle with the use of an elastic-viscous analogy. According to the elastic beam theory, the maximal deflection f of a beam submitted to a force F applied in its middle is :

$$f = \left[\frac{1}{4}\frac{Fl^3}{bh^3}\right]\frac{1}{E} \qquad (1)$$

where b, h, l are respectively the width, the height, the length of the beam and E is the Young modulus. For a linear viscous material with a viscosity ν, it is assumed that the deflection df during a time dt can be estimated by replacing in Equation 1 E by ν / dt. Thus the viscosity can be calculated along the thermal cycle by :

$$\nu(t) = \frac{Fl^3}{4bh^3\,(df/dt)} \qquad (2)$$

This procedure has been validated in a previous paper [12].

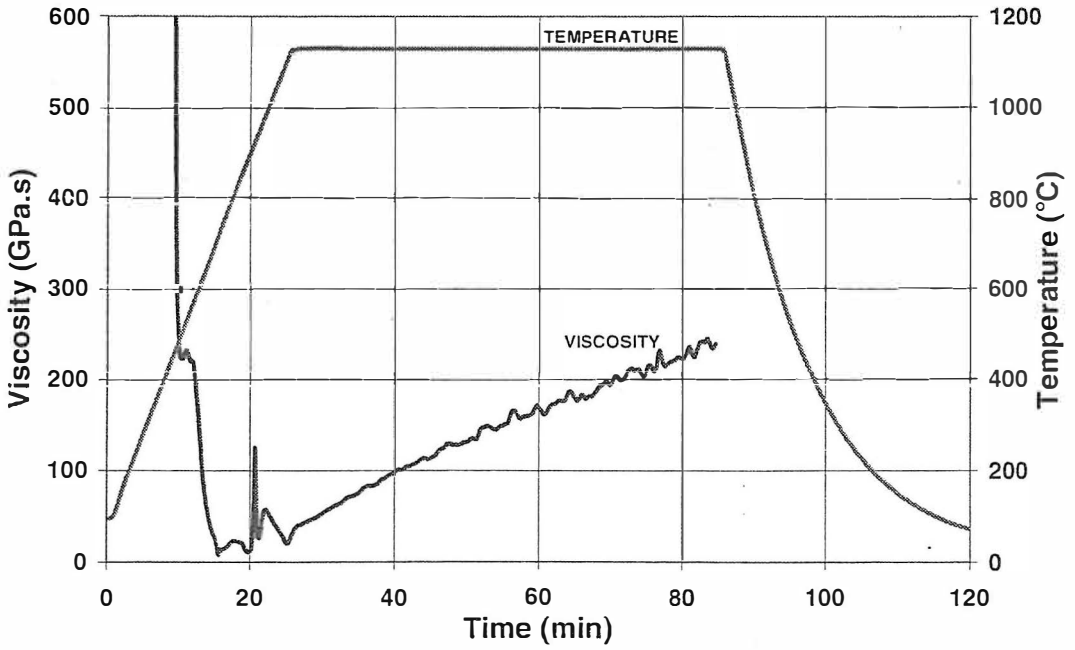

Figure 8. Viscosity of sample (a) measured during a bending test along a typical thermal cycle.

The result obtained for sample (a) is reported in Figure 8. During heating, two phenomena, with opposite effects on the viscosity, are simultaneous. As the temperature increases, the intrinsic viscosity of the material constituent of the particles decreases whereas interparticle contacts welding strengthen the

material. Globally, this results in a decrease of the viscosity with a lowest value about 10 GPa.s. Around 900°C, the $\alpha \rightarrow \gamma$ iron phase transformation occurs which produces apparently a stabilisation of the viscosity. During the sintering period at 1130°C, the viscosity continuously increases, likely as a consequence of the microstructural evolution of the material (diffusion of alloying elements leading in particular to the formation of steel phases). After one hour the viscosity is equal to 240 GPa.s.

The viscosity of sample (b) has been calculated with the same method. The result is reported in Figure 9. First of all, it can be observed that the order of magnitude of the viscosity is much higher than the values found for sample (a). In particular during the isothermal stage at 1130°C, the viscosity is around 2000 GPa.s , i.e.10 times higher than sample (a) at the same temperature. In addition, during the heating ramp, the viscosity decreases until the beginning of the phase transformation. During phase transformation, the viscosity increases. Then it decreases again as the temperature goes up until 1130°C.

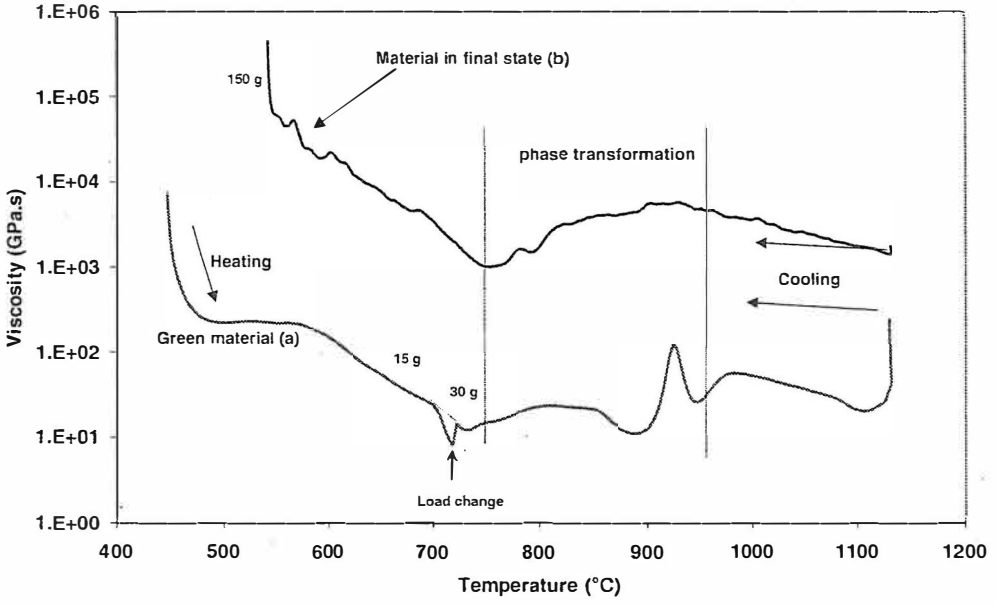

Figure 9. Viscosity of sample (a) compared to (b) as function of temperature measured during bending.

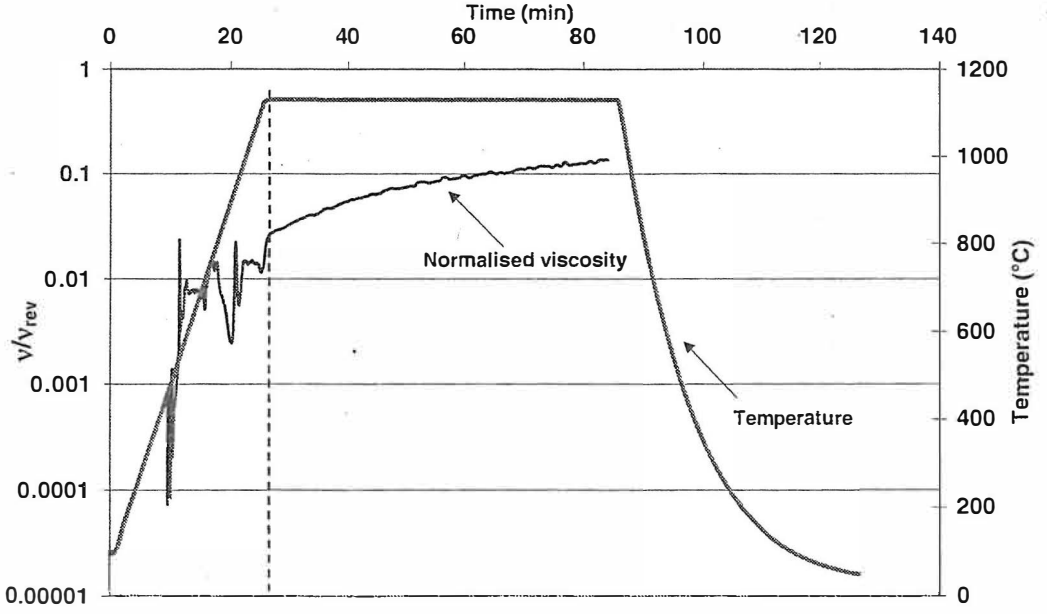

Figure 10. Normalised viscosity of sample (a)

The viscosity of sample (a) at a given temperature has then been normalised with regard to the viscosity of sample (b) at the same temperature (Figure 10), which provides a dimensionless parameter likely to characterise to progress of sintering. During the heating ramp, the normalised viscosity is multiplied by a factor of 100 in a very short time. This effect probably corresponds to the initial interparticle welding. Afterwards, the data obtained during period from the phase transformation to the isothermal period are very scattered. This result was expected from Figure 9. During the isothermal period, the normalised viscosity gently increases, from 0.03 to 0.13, i.e., at the end of the isothermal stage, the value of the normalised viscosity is around 0.13 which means that only 13 % of the final viscosity has been reached. It is then clear that the viscosity would keep increasing during several hours if the temperature were maintained.

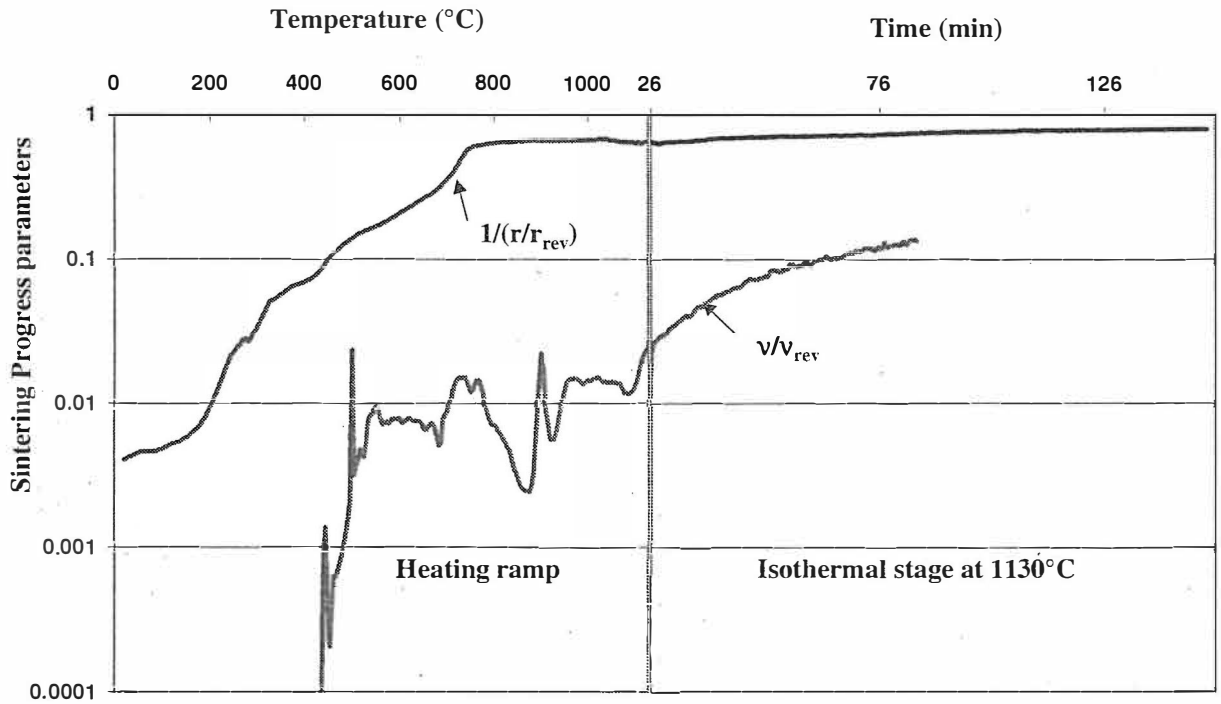

Figure 11 : Sintering progress parameter along the first thermal cycle.

DISCUSSION AND CONCLUSION

An innovative experiment device has been developed to measure both the shrinkage and the electrical resistivity of a material continuously during a thermal cycle. Moreover, an experimental procedure has been defined to submit a sintering compact to a bending test and an analytical method has been proposed to estimate the viscosity of the material from the data drawn from this test. Both tests have been performed with Distaloy AE powder compacts.

A dimensionless parameter has been deduced from the results of each test. In spite of some uncertainty on these results, both parameters seem to be relevant for characterising the irreversible changes of the material and thus the progress of sintering. Their changes throughout sintering are compared in Figure 11. The parameter deduced from resistivity measurement, which is supposed be related with the welding of contacting particles, shows a strong increase at low and intermediate temperature and is almost constant during isothermal sintering at 1130°C (+20 % in two hours). The parameter deduced from bending tests increases during both heating and isothermal periods. It is multiplied by 4 during one hour sintering at 1130°, which is likely a consequence of microstructural changes of the material related with the diffusion of alloying elements.

Both sintering progress parameters could be used for a macroscopic description of sintering. The physical interpretation of the variation of each one should be further investigated from the observation of microstructural changes of the material either by classical electron microscopy or better by advanced 3D imaging techniques as X-ray microtomography [13].

REFERENCES

[1] V.V. Skorokhod, " On the phenomenological theory in the sintering of porous bodies ", *Poroskova Metall.*, Vol 2, 1961, pp. 14-20.
[2] C.R. Reid, "Application of a continuum theory for sintering to densification rates", *Mechanics of Granular Materials and Powder Systems*, Proceeding of ASME., Vol. 37, 1992, pp. 19-27.
[3] C.R. Reid, "Numerical simulation of free shrinkage using a continuum theory for sintering", *Powder Tech.*, Vol 81, 1994, pp.287-291.
[4] E.A. Olevsky,"Theory of sintering : from discrete to continuum", *Mat. Sci. Eng. Report*, Vol R23(2), 1998.
[5] O. Lame, D. Bouvard and H. Wiedemann "Anisotropic shrinkage and gravity-induced creep during sintering of steel powder compacts", *Powder Met.*, Vol 45, No 1; 2002.
[6] A. Simchi, H. Danninger, "Electrical conductivity and microstructure of sintered ferrous materials: sintered iron", *Powder Met.*.,Vol. 43, No3, 2000, pp 209.
[7] A. Simchi, H. Danninger, B Weiss, "Microstructural modelling of electrical conductivity and mechanical properties of sintered ferrous materials", *Powder Met.*, Vol. 43, No 3, 2000, pp 219.
[8] A.Simchi, H.Danniger, and C Gierls, "Electrical conductivity and microstructure evolution of sintered ferrous materials : iron-graphite compacts" *Powder Met.*, Vol. 44, No 2, 2001, pp 148-156.
[9] L.P. Lefebre, G Pleizier, Y. Deslandes, "Electrical resistivity of green powder compacts" *Powder Met.*, Vol 44, No 3, 2001, pp 259-266.
[10] P. Z. Cai, G. L. Messing, D. J. Green, "Determination of the mechanical response of sintering compacts by cyclic loading dilatometry", *J. Am. Ceram. Soc.*, Vol 80, 1997, pp 445-452.
[11] O.Gillia, C.Josserond, D. Bouvard," Viscosity of WC-Co compacts during sintering " *Acta Mater.*,Vol 49, No 8, 2001, pp 1413-1420.
[12] O Lame and D Bouvard, "Viscosity measurements during sintering of iron-based compacts", *Proceeding of 2001 Powder Metallurgy World Congress*, Nice, France, EPMA, Shrewsbury UK.
[13] O. Lame, D. Bellet, M. Di Michiel and D. Bouvard, "In-situ microtomography of metal powder compacts during sintering", *Same proceedings.*